Pharmaceutical Research, Vol. 22, No. 8, August 2005 (© 2005)
DOI: 10.1007/s11095-005-5266-8

Research Paper

The Use of a Sum of Inverse Gaussian Functions to Describe the Absorption Profile of Drugs Exhibiting Complex Absorption

Chantal Csajka,[1] David Drover,[2] and Davide Verotta[1,3,4]

Received December 1, 2004; accepted March 23, 2005

Purpose. The aim of this study was to evaluate the utility of a parametric deconvolution method using a sum of inverse Gaussian functions (IG) to characterize the absorption and concentrations *vs.* time profile of drugs exhibiting complex absorption.
Methods. For a linear time-invariant system the response, Y(t), following an arbitrary input function I(t), is the convolution of I(t) with the disposition function, H(t), of the system: $Y(t) = \int_0^t I(\tau)H(t-\tau)d\tau$. The method proposed uses a sum of *n* inverse Gaussian functions to characterize I(t). The approach was compared with a standard nonparametric method using linear splines. Data were provided from previously published studies on two drugs (hydromorphone and veralipride) showing complex absorption and analyzed with NONMEM®.
Results. A satisfactory fit for hydromorphone and veralipride data following oral administration was achieved by fitting a sum of two or three IG functions. The predictions of the input functions were very similar to those using linear splines.
Conclusions. The use of a sum of IG as opposed to nonparametric functions, such as splines, offers a simpler implementation, a more intuitive interpretation of the results, a built-in extrapolation, and an easier implementation in a population context. Disadvantages are an apparent greater sensitivity to initial value estimates (when used with NONMEM®).

KEY WORDS: complex absorption; input model; inverse Gaussian functions; pharmacokinetics; splines.

INTRODUCTION

Drug absorption from the gastrointestinal tract is generally considered to occur by passive diffusion throughout the gastrointestinal membrane and a first- or zero-order absorption rate is commonly used to characterize drug absorption. However, for drugs whose absorption involves an active process via transporters, multiple absorption sites, or for drugs exhibiting an enterohepatic recycling, zero- or first-order absorption processes are unable to depict correctly the appearance of the drug in the blood stream (1). As a consequence of complex absorption rate profiles the corresponding plasma concentration–time profiles are irregular and cannot be interpreted easily using conventional models. Several methods have been proposed for the analysis of complex absorption. Nonparametric deconvolution methods, which were developed in the 1960s and achieved maturity in the early 1990s [see (2) for a comprehensive review], have played an important role. These methods are useful because they allow the characterization of arbitrarily complex input rate functions without making assumptions other than their belonging to a very flexible function class, such as splines (3). A different class of methods treat the absorption process as a discontinuous or a stepwise interrupted process (4–6). Some other methods have used more mechanistic models that incorporate a variety of physiological factors involved in the oral absorption process (7–9). Generally, flexible and simple parametric models that can be used to describe the complex process of drug input are lacking. This article presents an extension of the deconvolution method proposed by Weiss (10). The method uses a weighted sum of inverse Gaussian functions to represent the input function and can be used both for individual and population data. This article includes the following: (1) a description of the method, (2) a characterization of the input function of an extended-release formulation of hydromorphone using a sum of inverse Gaussian functions in population data (3) a description of the input and disposition functions of veralipride in individual data where the input function is represented by a sum of inverse Gaussian functions or (4) by linear splines, and (5) a comparison of the predictions and the estimates obtained for veralipride using inverse Gaussian functions and linear splines as input functions.

[1] Department of Biopharmaceutical Sciences, University of California, San Francisco, California 94143, USA.
[2] Department of Anesthesia, Stanford University School of Medicine, Stanford, California 94305, USA.
[3] Department of Biostatistics, University of California, San Francisco, California 94143, USA.
[4] To whom correspondence should be addressed. (e-mail: davide@ariel1.ucsf.edu)

MATERIALS AND METHODS

Theory

The output function at time t, $Y(t)$, of a linear time-invariant system is given by the convolution of the input function, $I(t)$, to the system with the disposition function, $H(t)$, of the system (2):

$$Y(t) = \int_0^t I(\tau)H(t-\tau)d\tau \tag{1}$$

where τ is an integration variable. Many methods have been presented to estimate $I(t)$ (2). We will use a maximum-likelihood approach, where given data following a known input (typically intravascular) and an unknown input (i.e., the absorption rate resulting from an extravascular administration) we estimate simultaneously or sequentially $I(t)$ and $H(t)$. To characterize $I(t)$ we propose to use a weighted sum of n inverse Gaussian functions: The j^{th} inverse Gaussian function, $IG_j(t)$, is defined by the following Eq. (10):

$$IG_j(t) = \sqrt{\frac{MAT_j}{2\pi CV_j^2 t^3}} e\left[-\frac{\left(t-MAT_j\right)^2}{2CV_j^2 MAT_j t}\right] \tag{2}$$

where MAT_j is the mean input rate time and CV_j^2 is the squared coefficient of variation ($CV_j = \frac{\sigma_j}{MAT_j}$, where σ_j^2 is the variance associated with $IG_j(t)$). An alternative parameterization that is useful in applications is the time to peak, $t_{\max}$, of $IG_j(t)$, which estimates the time at which the input rate attains its maximum value. Equation (2) was reparameterized as follows (10):

$$t_{\max j} = MAT_j\left[1 + \frac{9}{4}CV_j^4 - \frac{3}{2}CV_j^2\right] \tag{3}$$

instead of MAT_j. The j^{th} inverse Gaussian function now takes the following form:

$$IG_j(t) = \sqrt{\frac{t_{\max_j}/A}{2\pi CV_j^2 t^3}} e\left[-\frac{\left(t-t_{\max_j}/A\right)^2}{2CV_j^2 t_{\max_j}/At}\right] \tag{4}$$

where A is the part in brackets $1 + \frac{9}{4}CV_j^4 - \frac{3}{2}CV_j^2$ of Eq. (3).

The input function can be represented using a sum of inverse Gaussian functions as follows:

$$I(t) = FD\sum_{j=1}^{n} f_j IG_j(t) \tag{5}$$

where ${}_n F$ denotes the bioavailability, D the administered dose, $\sum_{j=1} f_j = 1$ (note that $\int_0^\infty IG_j(\tau)d\tau = 1, j = 1, \ldots, n$, therefore $\sum_{j=1}^m \int_0^\infty f_j IG_j(\tau)d\tau = \sum_{j=1}^m f_j = 1$). This parameterization (referred to in the following as P1) offers the advantage that the parameter F is estimated directly. An alternative parameterization (P2) is the following:

$$I(t) = D\sum_{j=1}^{n} f_j IG_j(t) \tag{6}$$

where now $0 \le \sum_{j=1}^{n} f_j \le 1$, and the bioavailability is derived as $F = \sum_{j=1}^{n} f_j$.

For methodologies comparison the input function was also characterized using a linear spline, which is represented using B-splines bases function (3):

$$I(t) = D\sum_{j=1}^{m} \alpha_j B_j(t) \tag{7}$$

where m is the number of basis functions $B_j(t)$ and α_j are parameters to be estimated. The breakpoints of the spline were put at time zero (ξ_1) and at the quantiles of the observations times for the extravascular administration (ξ_j $j = 2, \ldots, m$). For easy reference we report the expression for the B-spline basis functions [see (11) for details]. The B-splines functions have the shape of triangles:

$$\text{For } j = 1 \begin{cases} B_1(t) = \dfrac{\xi_{j+1} - t}{\left(\xi_{j+1} - \xi_j\right)} & \xi_j \le t \le \xi_{j+1} \\ 0 & \text{otherwise} \end{cases} \tag{8}$$

$$\text{For } j = 2, \ldots, m-1 \begin{cases} B_j(t) = \dfrac{t - \xi_{j-1}}{\xi_j - \xi_{j-1}} & \xi_{j-1} \le t \le \xi_j \\ B_j(t) = \dfrac{\xi_{j+1} - t}{\xi_{j+1} - \xi_j} & \xi_j \le t \le \xi_{j+1} \\ 0 & \text{otherwise} \end{cases} \tag{9}$$

$$\text{For } j = m \begin{cases} B_m(t) = \dfrac{t - \xi_{m-1}}{\xi_m - \xi_{m-1}} & \xi_{m-1} \le t \le \xi_m \\ 0 & \text{otherwise} \end{cases} \tag{10}$$

The bioavailability F is derived as the time integral of the input:

$$\int_0^{\xi_m} I(\tau)d\tau = \xi_1\alpha_1/2 + \sum_{j=1}^{m-1}\left(\xi_{j+1} - \xi_{j-1}\right)\frac{\alpha_j}{2} + \xi_m\alpha_m/2 \tag{11}$$

Note that the representation of $I(t)$ just described is zero outside the interval $[\xi_1, \xi_m]$: a spline representation does not provide a built-in extrapolation.

Data

The analysis was based on data gathered from two studies in healthy volunteers previously described in (12) and (5).

Hydromorphone

Briefly stated, the first study was a randomized crossover design study, in which 12 volunteers received hydromorphone 8 mg intravenous; 8 mg in an immediate-release (IR) oral form (Dilaudid®, Abbott Laboratories, Abbott Park, IL); and 8 mg, 16 mg, and 32 mg of an extended release formulation (OROS®, Abbott Laboratories). The OROS® formulation is a sustained release system that uses a semipermeable membrane around a drug tablet core which is capable of providing sustained drug release once swallowed orally. Arterial blood samples after administration of the

Table I. Estimates of the Pharmacokinetic Parameters for Hydromorphone

	Population mean		Intersubject variability[a]	
	Estimates	SE (%)[b]	Estimates	SE (%)[b]
t_{max1} (min)	251	6		
t_{max2} (min)	784	3	7%	60
t_{max3} (min)	1790	7		
CV_1	0.464	10		
CV_2	0.303	13	0%	—
CV_3	0.378	15		
F	0.27	7	25%	41
f_1	0.11	9		
f_2	0.39	9		
σ (CV%)[c]	36%	12		

t_{max1}, t_{max2}, t_{max3}, time at maximum input rate; CV_1, CV_2, CV_3, normalized variance of the distribution associated with each inverse Gaussian function; F, bioavailability; and f_1, f_2, the fractional input associated with each function.
[a]Estimates of variability expressed as a coefficient of variation (CV%).
[b]Standard error of the estimates (SE), defined as SE/estimate expressed as a percentage.
[c]Residual intrasubject variability expressed as coefficient of variation (CV%).

infusion were drawn immediately before the dose and at 1, 3, 5, 7, 10, 11, 12, 13, 15, 17, 20, 25, 40, 55, 70, 100, 130, 190, 250, 370, 490, 730, 970, and 1450 min after drug administration. Venous blood samples after administration of the OROS® formulations were drawn before the dose and at 1, 2, 3, 6, 9, 12, 15, 18, 21, 24, 30, 36, and 48 h after drug intake. All the data were considered in a population data analysis.

Veralipride

The second study involved veralipride. In this study, 12 healthy volunteers received three different pharmaceutical forms of veralipride—a 30-min constant intravenous infusion, an oral solution, and a capsule- at 1-week intervals in a randomized crossover design. In each case, a 100-mg dose was administered in the morning after an overnight fast. Plasma sampling was done immediately before the dose and at 0.17, 0.33, 0.5, 0.75, 1, 1.5, 2, 2.5, 3, 4, 6, 8, 10, 12, and 24 h after drug administration. The absorption profile following the administration of the oral solution of veralipride is characterized by a double-peak phenomenon. To illustrate the application of our method, two subjects were chosen who exhibited a marked double absorption peak, and one subject who showed a smaller second peak.

Model-Based Analysis

Hydromorphone

OROS® hydromorphone deconvolution was performed sequentially. The disposition parameters were fixed to the individual empirical Bayesian disposition estimates provided by our previous study, in which a three-compartment model was used to fit the intravenous data (12). The absorption rate was then modeled using a sum of inverse Gaussian functions. The model is described by the following differential equations:

$$\frac{dA_1}{dt} = k_{21}A_2 + k_{31}A_3 - (k_{10} + k_{12} + k_{13})A_1 + I(t) \quad (12)$$

$$\frac{dA_2}{dt} = k_{12}A_1 - k_{21}A_2 \quad (13)$$

$$\frac{dA_3}{dt} = k_{13}A_1 - k_{31}A_3 \quad (14)$$

$$C(t) = \frac{A_2(t)}{V} \quad (15)$$

where A_1, A_2, and A_3 are the amounts in the central and the two peripheral compartments, respectively; k_{xy} is the transfer rate constants from compartment x to compartment y (y = 0 when it denotes the outside of the compartmental model); $I(t)$ is the sum of two or three inverse Gaussian functions as described in Eq. (5), parameterized in terms of MAT [Eq. (2)] or t_{max} [Eq. (4)].

Veralipride

The modeling of veralipride deconvolution was performed with a simultaneous approach, allowing the disposition and the input functions to be characterized during the same analysis. A two-compartment model was used to model the data, as previously reported (5). Each of the three subjects was modeled separately, using either inverse Gauss-

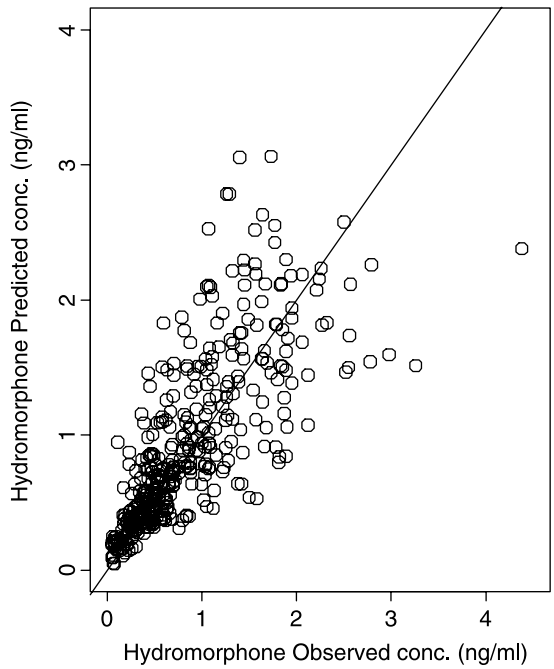

Fig. 1. Predicted *vs.* observed hydromorphone concentrations in 12 subjects after administration of both 8 mg intravenously and 8, 16, and 32 mg orally in an OROS® formulation.

ian functions or linear splines to represent the input rate function. The model is expressed using differential equations as follows:

$$\frac{dA_1}{dt} = k_{21}A_2 - (k_{10} + k_{12})A_1 + I(t) \tag{16}$$

$$\frac{dA_2}{dt} = k_{12}A_1 - k_{21}A_2 \tag{17}$$

where $I(t)$ is the sum of two or three inverse Gaussian functions parameterized in terms of t_{max} [Eqs. (4) and (5) or by the linear splines [Eqs. (10)–(13)].

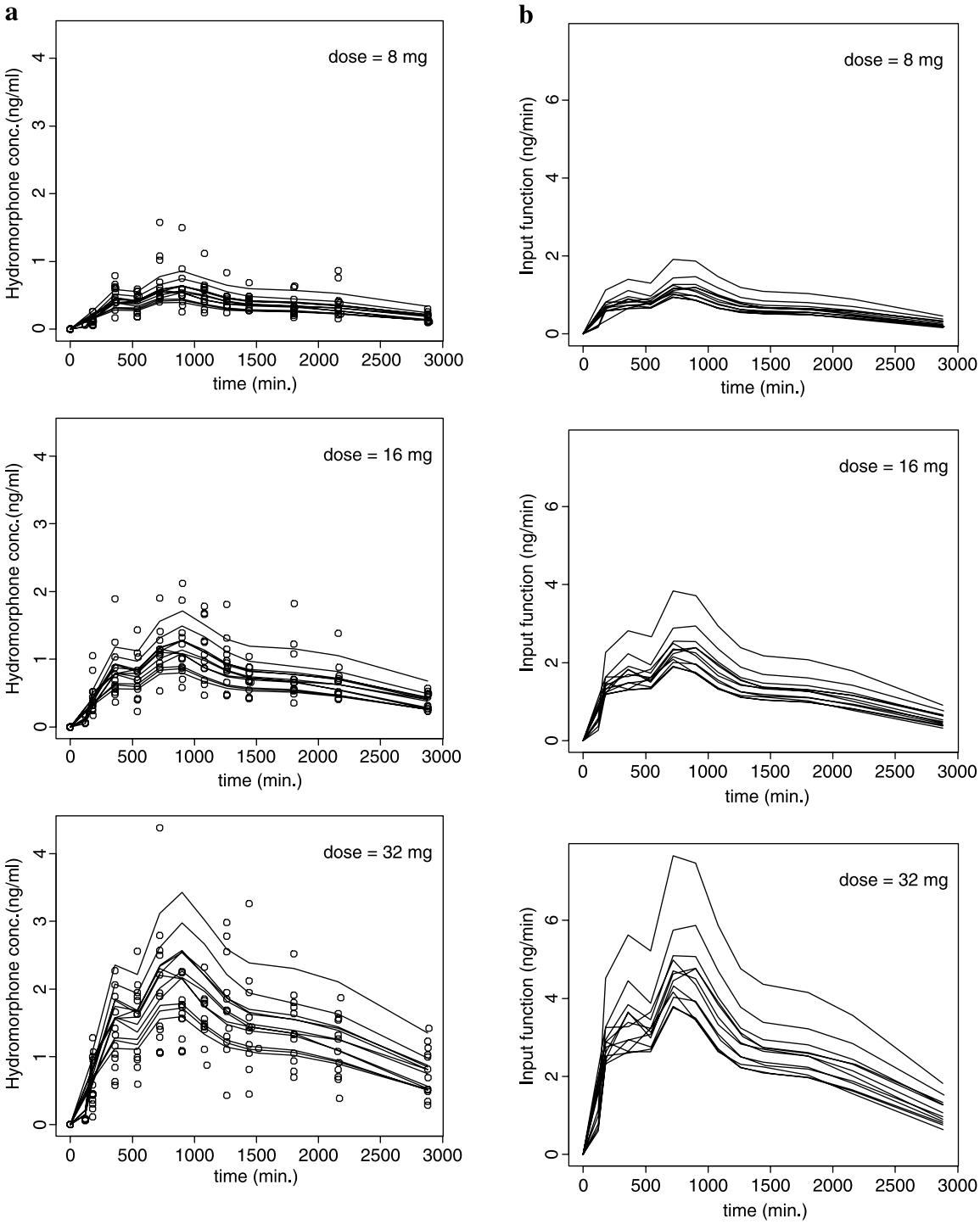

Fig. 2. (a) Plasma concentrations (open circles) and individual predictions (solid line) *vs.* time for OROS® hydromorphone after administration of the 8-mg (upper panel), the 16-mg (middle panel), and the 32-mg dose regimens (lower panel). (b) Individual input rate function *vs.* time after administration of the 8-mg (upper panel), the 16-mg (middle panel), and the 32-mg dose regimens (lower panel).

Statistical Models

Different models for intersubject variability can be used with a sum of inverse Gaussian functions. Only two such models are mentioned here. The first is the "saturated" model, which assigns a random-effect to each parameter of the model. Thus, for the i^{th} individual, we have the following:

$$\text{Using parametrization } P1 \text{ or } P2, \text{ for } j = 1, \ldots, n$$
$$MAT_{ij} = MAT_j e^{\eta_{i,j}}, \quad \text{or } t_{\max_{ij}} = t_{\max_j} e^{\eta_{i,j}} \qquad (18)$$
$$CV_{ij} = CV_i e^{\eta_{i,n+j}}$$

Using parametrization $P1$

$$F_i = F e^{\eta_{i,2n}}$$
$$\text{for } j = 1, \ldots, n-1$$
$$f_{ij} = f_i e^{\eta_{i,2n+1+j}}, \text{ and } f_{in} = 1 - \sum_{j=1}^{n-1} f_{ij}$$

$$\text{Using parametrization } P2 \quad \text{for } j = 1, \ldots, n$$
$$f_{ij} = f_i e^{\eta_{i,2n+j}}$$

The total number of random effects in this saturated model is $3 \times n$, where n is the number of inverse Gaussian functions. At the individual levels, we impose the same constraint of F and f_i described earlier; for example, $0 \le F_i \le 1$. This can be done in NONMEM using an EXIT statement. A useful sub-saturated model assumes that mean absorption times, coefficient of variation (CV), and bioavailability are each scaled by the same random effect. The model has a total of three random effects parameters, as follows:

$$\text{Using parametrization } P1 \text{ or } P2, \text{ for } j = 1, \ldots, n$$
$$MAT_{ij} = MAT_j e^{\eta_{i,1}}, \quad or\, t_{\max_{ij}} = t_{\max} \mathrm{e}^{\eta_{i,1}} \qquad (19)$$
$$CV_{ij} = CV_i e^{\eta_{i,2}}$$

$$\text{Using parametrization } P1 \quad F_i = F e^{\eta_{i,3}}$$

$$\text{Using parametrization } P2, \text{ for } j = 1, \ldots, n \quad f_{ij} = f_j e^{\eta_{i,3}}$$

As is usually done in population modeling, stepwise addition or deletion can also be used to add (starting from the sub-saturated model) or subtract (starting from the saturated model) random effects sequentially, keeping or removing the ones considered statistically significant.

We used a proportional error model to describe intra-individual (residual) variability for both hydromorphone and veralipride plasma concentrations. For the generic response Y and the corresponding prediction $\hat{Y}$, the k^{th} measurement for the ith individual takes the following form:

$$Y_{ki} = \hat{Y}(1 + \varepsilon_{ki}) \qquad (20)$$

where ε_{ki} is independent normally distributed with mean zero and a variance σ^2.

Implementation Details

Using NONMEM® (13), the parameters f_j in Eq. (5) were estimated using the following:

$$f_1 = \theta_1, f_j = \left(1 - \sum_{i=1}^{j-1} f_i\right)\theta_j, \; f_n = 1 - \sum_{i=1}^{n-1} f_i \qquad (21)$$

Table II. Estimates of the Pharmacokinetic Parameters for Veralipride in Three Subjects

	Subject 1				Subject 2				Subject 3			
	Inverse Gaussian		Splines		Inverse Gaussian		Splines		Inverse Gaussian		Splines	
	Estimates	SE[a]	Estimates	SE[a]	Estimates	SE[a]	Estimates	SE[a]	Estimates	SE[a]	Estimates	SE[a]
V (L)	22.1	43%	23.0	41%	17.5	7%	17.5	8%	27.3	9%	27.4	9%
k_{10} (h^{-1})	1.79	39%	1.72	37%	1.60	7%	1.59	8%	1.17	9%	1.17	9%
k_{12} (h^{-1})	5.15	44%	4.79	44%	5.8	11%	5.9	12%	3.49	10%	3.46	11%
k_{21} (h^{-1})	1.45	17%	1.42	18%	1.0	9%	1.0	9%	0.78	8%	0.78	8%
F	0.80	7%	0.81	23%[c]	0.72	5%	0.69	13%[c]	0.91	5%	0.59	10%[c]
$t_{\max 1}$ (h)	0.13	22%			0.11	13%			0.16	9%		
CV_1	1.09	11%			1.0	24%			0.86	13%		
$t_{\max 2}$ (h)	2.47	17%			2.16	17%			1.56	3%		
CV_2	0.24	34%			0.77	22%			0.22	19%		
$t_{\max 3}$ (h)	—				—				0.90	9%		
CV_3	—				—				40	7%		
f_1	0.84	5%			0.25	12%			0.085	21%		
f_2	0.16	—			0.75	—			−0.062	20%		
f_3	—	—			—	—			0.977	—		
σ^b	28%	45%	29%		10%	17%	9%		9%	27%	9%	

V, volume of distribution of the central compartment; kxy, transfer rate constant from compartment x to y; F, bioavailability; for each inverse Gaussian function, respectively; $t_{\max 1}$, $t_{\max 2}$, $t_{\max 3}$, time to maximal concentrations; and f_1, f_2, f_3, fractional input rate.
[a] Standard error of the estimates (SE), defined as SE/estimate expressed as a percentage.
[b] Estimates of residual variability expressed as a coefficient of variation (CV%)
[c] Derived from $\sum_{j=1}^{m} \frac{(\xi_{j+1} - \xi_{j-1})}{2} \mathrm{SE}(\alpha_j)$, where $\mathrm{SE}(\alpha_j)$ is the standard error of the estimate of the parameter α.

where $0 \le \theta_j \le 1$, $j = 1, \ldots, n$. We also imposed the constraint $MAT_1 \le MAT_2 \le \ldots \le MAT_n$ using the following:

$$MAT_1 = \theta_1, MAT_j = MAT_j + \theta_j, \quad \theta_j \ge 0 \qquad (22)$$

so that the inverse Gaussian functions are naturally ordered by MAT_j. For the population case, using the saturated model for example, the intersubject variability model Eq. (18) similarly imposes: $t_{\max ij} \ge t_{\max i,j-1}$, using $t_{\max ij} = t_{\max i,j-1} + \theta_j e^{\eta_{i,j}}$ for $j = 2, \ldots, n$.

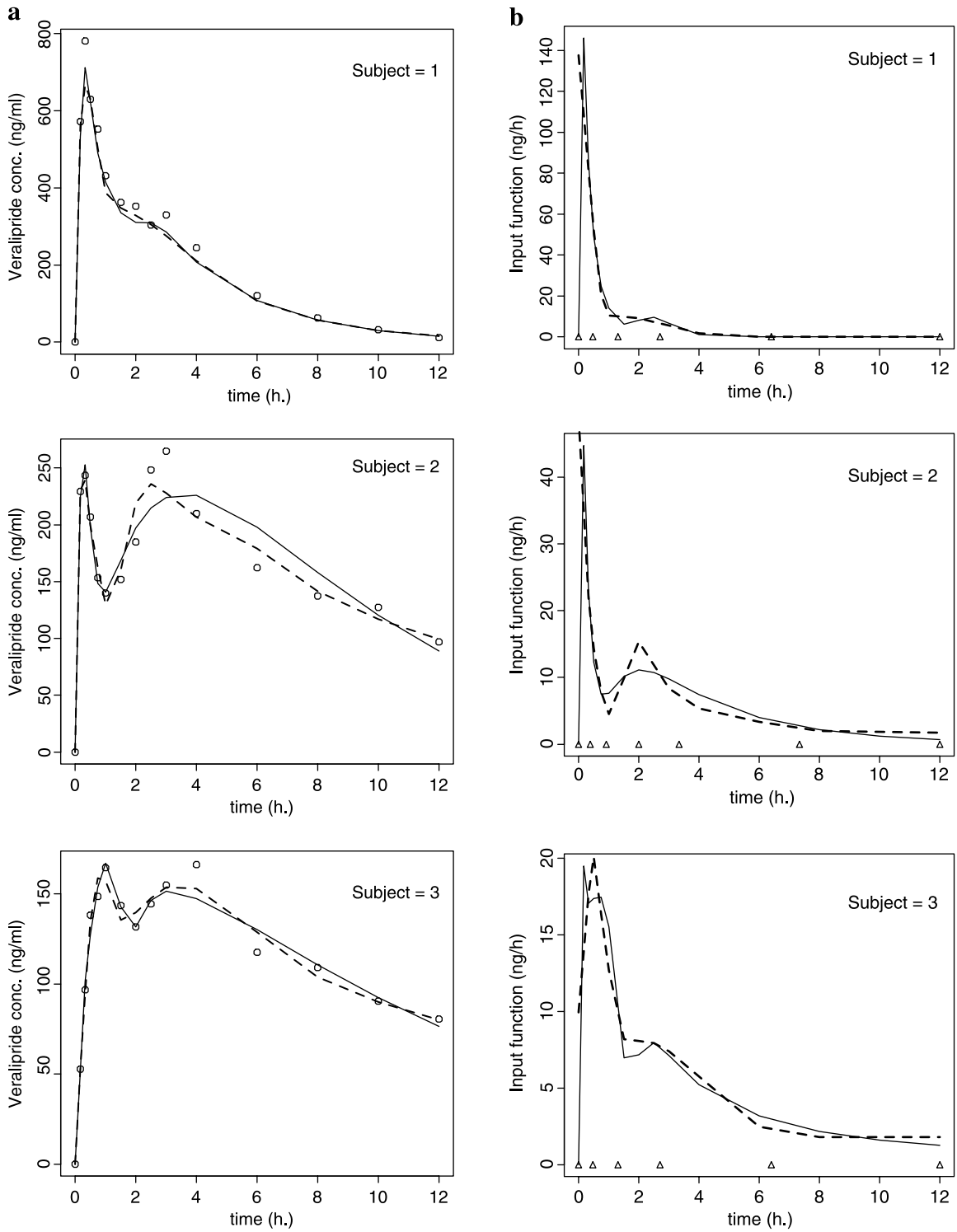

Fig. 3. (a) Plasma concentrations (open circles) and predictions using the sum of the inverse Gaussian functions (solid line) and the linear splines (dashed lines) after administration of 100 mg of veralipride in Subject 1 (upper panel), Subject 2 (middle panel), and Subject 3 (lower panel). (b) Individual input rate function *vs.* time for the three subjects using the sum of the inverse functions (solid line) or the linear splines (dashed lines) as input functions.

Parameter Estimation and Model Selection

Hydromorphone and veralipride concentration-time curves were analyzed by nonlinear regression using NONMEM VI (13) with the first-order (FO) method and three significant digits to fit the models described above to the data. The compiler is the SunPro FORTRAN 77 running on a Sun Workstation Ultra-5. NONMEM performs linearized maximum likelihood estimation by use of an objective function (OBJ). To determine the statistical significance between two models, different statistical selection criteria can be used (14–16) that require a minimal decrease of 2 to 10 points in the objective function (minus twice the logarithm of the linearized maximum likelihood of the model) to accept a model with one additional parameter. For both methods described earlier we increased n and m until the statistical model selection criterion fails to decrease. We also compared standard regression diagnostic plots. The figures were generated with S-PLUS (17).

RESULTS

Hydromorphone

The first analysis presents the results of a population study on hydromorphone, administered intravenously and as an OROS® formulation. The disposition parameters were fixed to the individual empirical Bayesian disposition estimates, which were shown to fit the intravenous data adequately with the use of a three-compartment model (12). One and a sum of two and three inverse Gaussian functions were tested as input functions. One input function did not describe the data appropriately, and showed a marked trend in the regression plots. The addition of a second inverse Gaussian function improved the fits (the decrease in the objective function was $\Delta OBJ = -150$). A sum of three inverse Gaussian functions provided an additional decrease in the objective function ($\Delta OBJ = -58$) and was able to capture the complex absorption profile with more flexibility. As expected, using either parameterisation with MAT [Eq. (2)] or t_{max} [Eq. (4)] resulted in a similar overall goodness of fit in the plots (not shown), but a significant drop in the OBJ ($\Delta OBJ = -8$) was noticed while estimating t_{max} rather than MAT.

Using the saturated model for inter-individual variability [Eq. (18)], only variabilities on t_{max1}, t_{max2}, t_{max3}, F, and f_2 could be estimated, whereas the variances for the other parameters were not statistically significantly different from 0. Using the sub-saturated model revealed inter-individual variabilities on F and on t_{max}, but the variance on $CV1$ was zero. In relation to these results, the model in which a variance was tested on each parameter sequentially was not relevant. Table I presents the final population estimates and coefficients of variation for hydromorphone using the parameterization $P1$ and the sub-saturated model for inter-subject variability. The plot of the observations *vs.* predictions is shown in Fig. 1. Figure 2a depicts the observed concentrations (open circles) *vs.* time with the individual predictions (solid line) obtained at each observed time points. Figure 2b presents the corresponding input functions, after administration of 8 mg (upper panel), 16 mg (middle panel), and 32 mg (lower panel) of hydromorphone.

Veralipride

The modeling of veralipride deconvolution was performed with a simultaneous approach, which allowed the disposition and the input functions to be characterized during the same analysis. A two-compartment model was used to model the data as previously reported (5). The use of a single inverse Gaussian function did not capture the two-peak phenomenon adequately. A sum of two inverse Gaussian functions statistically improved the fit of all three subjects compared to the model involving a single function ($\Delta OBJ = -4$, -83, and -31, respectively). Using a sum of three inverse Gaussian functions further decreased the objective function for Subject 3 ($\Delta OBJ = -18$), but did not improve the description of data for Subject 1 or 2 ($\Delta OBJ = 0$ for both subjects).

For comparison, linear splines were used to model the input function of the same three subjects. The use of six breakpoints at times 0, 0.46, 1.3, 2.7, 6.4, and 12.1 hours was first tested. The absorption data from all three subjects were characterized adequately by linear splines and six breakpoints. The use of seven breakpoints at times 0, 0, 0.386, 0.916, 2, 3.33, 7.33, and 12.1 h slightly improved the fit of Subject 2 ($\Delta OBJ = -4$), but did not further modify the input profile of Subject 1 or 3 ($\Delta OBJ = -0.8$ and 0, respectively). The parameter estimates for the absorption and disposition of veralipride using both a sum of inverse Gaussian functions and the linear splines as input functions are presented in Table II. Figure 3a shows the concentrations (open circles) for Subjects 1, 2, and 3 after administration of 100 mg of veralipride, with the prediction obtained using the inverse Gaussian function (solid line) and the linear splines (dashed lines). Figure 3b presents the corresponding predicted input functions using the sum of the inverse Gaussian functions (solid line) or linear splines (dashed lines).

DISCUSSION

Oral administration of drug is a very complex process that manifests itself trough potential interaction with a host of physicochemical and physiological variables. Factors that can potentially contribute to irregularities in drug absorption include presystemic metabolism/efflux, gastric pH/emptying rate, gastrointestinal motility, luminal contents, and formulation effects. Also, new drug formulations are being developed to make patient dosing easier and to improve drug effect, tolerance, and patient compliance. Using extended-release systems can produce complex absorption patterns that cannot be described effectively by the traditional sum-of-exponentials models. The typical first-order or zero-order absorption models are often not satisfactory mathematical models when drug release, absorption, and elimination occur simultaneously and in a complex fashion.

In this article, we suggest the use of a sum of inverse Gaussian functions to represent the input function of drugs exhibiting atypical drug absorption. We elaborate the method first presented by Weiss using a single inverse Gaussian function (10), and propose a novel approach, which uses a sum of inverse Gaussian functions and allows the representation of more complex absorption functions as shown by the examples reported in the preceding. To deal with the correspondingly more complex estimation problem (each

inverse Gaussian function adds three parameters) we introduce a parameterization in t_{max}. This allows a natural ordering of the functions, avoids flip-flops between the inverse Gaussian, and generally obtains slightly lower objective function values using NONMEM®, which is an indication of a more efficient minimization since, of course, the final values of OBJ should be identical and independent of parameterization.

Our results show that a sum of three inverse Gaussian functions is necessary to describe the absorption profile of OROS® hydromorphone, which shows a very complex absorption pattern. We obtained population estimates of t_{max1} = 251, t_{max2} = 784 and t_{max3} = 1790 for the successive peaks of the input observed after administration of OROS® hydromorphone, as shown in Fig. 2. The estimated bioavailability of 0.27 is in close agreement with the bioavailability calculated from the area under the input rate *vs.* time curve using linear splines in our previous analysis (F = 0.24, SD = 0.06) (12).

The concentration–time profile of veralipride, whose absorption profile is characterized by a marked double-peak phenomenon, was characterized as well by a sum of two or three inverse Gaussian functions, as shown Fig. 3a. The comparison to a previous analysis of veralipride which used a two-site absorption model (5) showed that the estimated $t_{max2} = 2.47$ h for Subject 2 is in good agreement with the reported value of 2.53 h. As opposed to their model that could not find an acceptable solution for Subject 1, the sum of inverse Gaussian functions was able to detect a two-peak phenomenon. The second peak was, however, small in this individual and slightly underpredicted. For Subject 3, one of the weights of the inverse Gaussian functions is negative (although the input function is non-negative everywhere); thus the values of t_{max} reported in Table II do not correspond to times of successive peaks visible in the input *vs.* time plot. For comparative purposes, we estimated graphically peaks at 0.7, and 2.5 h. These values are very similar to the values 0.99 and 2.53 h reported in (5). The bioavailability F = 0.81, 0.69 and 0.91 for Subjects 1, 2, and 3, respectively, are close to the mean reported value of F = 0.86 (SD = 0.31). [The data analyst should be aware that the weight attached to each inverse Gaussian function is not constrained to be positive, but that at any time the $I(t) = D\sum_{j=1}^{n} f_j IG_j(t)$ term should be non-negative, to be consistent with physiology. Thus a fit resulting in a negative input function should be rejected, the exception is for special situations in which the input function can become negative, e.g., after charcoal administration following an oral dose (18)].

The comparison of the sum of inverse Gaussian method with a nonparametric approach shows (Fig. 3a, b) that the concentrations–time profile and the input-time profile using linear splines (dashed lines) are very similar to those represented by inverse Gaussian functions (solid lines). The only notable difference is the 35% lower bioavailability estimated in Subject 3 using the linear splines. The lack of extrapolation using a nonparametric approach, as opposed to the presence of a built-in extrapolation using inverse Gaussian functions, might explain the discrepancy in F observed for this individual, whose terminal slope appears particularly flat.

Compared to other nonparametric functions, such as splines, this approach offers the advantage that it is parametric and that the results can be directly related to the absorption process, that is, F, MAT_j, or t_{maxj} the mean absorption times or times of maximal input rate; the parameter *CV*1 can be related to the dispersion of the shape of the absorption profile. This approach also offers a simpler and more easily interpretable implementation in a population context. One of the main disadvantages when using a nonparametric method in a population context is indeed that the issue of associating intersubject variability to the structural model using random effects is not trivial (11). In the case of a parametric model random effects are naturally associated with the model parameters. For a nonparametric model, however, such as a spline, the parameters offer little, if any, interpretation, thus complicating the interpretation of random effects when associated with the parameters of the spline. The number of parameters in a spline is generally very high, which makes associating random effects to each parameter (thus generating a "saturated" random effect model) impractical. Moreover, it is not straightforward to use "subsaturated" models, in which random effects are not associated with each parameter of the spline. Possible ways to correct these problems, and fully describe inter-individual variability associated with a nonparametric model, are described in (11). Compared to the splines, we observed that this model had the disadvantages of an apparent greater sensitivity to initial value estimates, leading to termination of the minimization at multiple apparent local minima. This is very common when using nonlinear models in NONMEM, and we recommend constraints and choosing multiple reasonable initial estimate, to identify the (apparent) minimum of the objective function.

Although this method does not propose an underlying mechanism of absorption, we have shown that it could be used to characterize irregularities in absorption arising from different sources. In addition, a reviewer suggests that it could also be used for gastric emptying-limited absorption, enterohepatic cycling, or window-type absorption; see (19) for a review of these phenomena. In the case of a window-type absorption process, when an "absorption window" may exist within the gastrointestinal tract, multiple lag times could simply be introduced in the model to characterize delays in reaching the most effective absorption site. That is, one can use

$$IG_j^*(t) = \begin{cases} 0, t \le t_{\text{lag},j} \\ IG_j\left(t - t_{\text{lag},j}\right), \text{otherwise} \end{cases}$$

where $t_{\text{lag},j}$ is the lag time for the j^{th} inverse Gaussian function. A single lag time, similar to what is commonly used with a first-order absorption function, is simply achieved by constraining $t_{\text{lag},1} = t_{\text{lag},2} = \ldots t_{\text{lag},n}$. The constraint $t_{\text{lag},1} \le t_{\text{lag},2} \le \ldots t_{\text{lag},n}$ achieves differential lag-times between the inverse Gaussian functions, thus allowing differential starting points for multiple absorption process (we remark that in the case of absorption windows constraints such as $MAT_1 \le MAT_2 \le \ldots \le MAT_n$ might not be appropriate, since absorption characteristics corresponding to multiple well separated absorption sites might not need to be ordered.)

ACKNOWLEDGMENT

This study was supported by NIH Grant A150587.

REFERENCES

1. L. F. Prescott. Gastrointestinal absorption of drugs. *Med. Clin. N. Am.* **58**:5–17 (1974).
2. D. Verotta. Concepts, properties and applications of linear systems to describe distribution, identify input, and control endogenous substances and drugs in biological systems. *Crit. Rev. Biomed. Eng.* **24**:73–139 (1996).
3. C. DeBoor. *A Practical Guide to Spline*, Springer-Verlag, New York, 1978.
4. K. Ishii, Y. Katayama, S. Itai, Y. Ito, and H. Hayashi. A new pharmacokinetic model including *in vivo* dissolution and gastrointestinal transit parameters. *Biol. Pharm. Bull.* **18**(6): 882–886 (1995).
5. Y. Plusquellec, G. Campistron, S. Staveris, J. Barre, L. Jung, J. P. Tillement, and G. Houin. A double-peak phenomenon in the pharmacokinetics of veralipride after oral administration: a double-site model for drug absorption. *J. Pharmacokinet. Pharmacodyn.* **15**(3):225–239 (1987).
6. R. Suverkrup. Discontinuous absorption processes in pharmacokinetic models. *J. Pharm. Sci.* **68**:1395–1400 (1979).
7. K. Murata, K. Noda, K. Kohno, and M. Samejima. Pharmacokinetic analysis of concentration data of drugs with irregular absorption profiles using multi-function absorption models. *J. Pharm. Sci.* **76**:109–113 (1987).
8. K. Higaki, S. Yamashita, and G. L. Amidon. Time-dependent oral absorption models. *J. Pharmacokinet. Pharmacodyn.* **28**(2):109–128 (2001).
9. R. L. Oberle and G. L. Amidon. The influence of variable gastric emptying and intestinal transit rates on the plasma level curve of cimetidine: an explanation for the double peak phenomenon. *J. Pharmacokinet. Biopharm.* **15**:539–544 (1987).
10. M. Weiss. A novel extravascular input function for the assessment of drug absorption in bioavailabilities studies. *Pharm. Res.* **13**(10):1547–1553 (1996).
11. K. E. Fattinger and D. Verotta. A nonparametric subject-specific population method for deconvolution: I. Description, internal validation, and real data examples. *J. Pharmacokinet. Biopharm.* **23**(6):581–610 (1995).
12. D. R. Drover, M. S. Angst, M. Valle, B. Ramaswamy, S. Naidu, D. R. Stanski, and D. Verotta. Input characteristics and bioavailability after administration of immediate and a new extended-release formulation of hydromorphone in healthy volunteers. *Anesthesiology* **97**:827–836 (2002).
13. A. J. Boeckmann, S. L. Beal, and L. B. Sheiner. *NONMEM Users' Guides*, NONMEM Project Group, University of California at San Francisco, San Francisco, http://www.globomax.net/products/nonmem.cfm, 1992.
14. A. Akaike. A new look at the statistical model identification problem. *IEEE Trans. Automat. Contr.* **19**:716–723 (1974).
15. E. J. Hannan. Rational transfer function approximation. *Stat. Sci.* **2**:1029–1054 (1987).
16. G. Schwartz. Estimating the dimension of a model. *Ann. Stat.* **6**:461–464 (1978).
17. S-Plus Software, Statistical Sciences, Version 4.0 Release 2, 1997. http://www.statsci.org/splus.html.
18. P. Veng-Pedersen, M. J. Berg, and D. D. Schottelius. Linear system approach for the analysis of an induced drug removal process. Phenobarbital removal by oral activated charcoal. *J. Pharmacokinet. Biopharm.* **14**:19–28 (1986).
19. H. Zhou. Pharmacokinetic strategies in deciphering atyptical drug absorption profiles. *J. Clin. Pharmacol.* **43**:211–227 (2003).